

## Molecular-dynamics study of the structural rearrangements of Cu and Au clusters softly deposited on a Cu(001) surface

F. J. Palacios, M. P. Iñiguez, M. J. López, and J. A. Alonso  
*Departamento de Física Teórica, Universidad de Valladolid, 47011 Valladolid, Spain*  
 (Received 1 February 1999)

The soft deposition of copper and gold clusters on the Cu(001) surface is studied by constant energy molecular-dynamics simulations. The atomic interactions are mimicked by a many-body potential based on the tight-binding model. The influence of cluster size, substrate temperature, and incident kinetic energy (in the low-energy limit) is analyzed. Some of the simulations are extended up to a few hundred picoseconds and within this simulation time the cluster flattens and partially spreads over the surface, and the degree of spreading depends on the above variables. The influence of surface steps has also been studied and the deposited atoms seem to have a strong affinity for step-edge sites. [S0163-1829(99)14227-9]

### I. INTRODUCTION

The fabrication of atomic nanostructures on surfaces opens up new possibilities for technological applications. These structures can be observed by STM (scanning tunneling microscopy)<sup>1-4</sup> and the different mechanisms that control their production have associated different characteristic speeds which also depend on the experimental conditions. Clusters of nanometric dimensions and various morphologies are produced by diffusion-controlled aggregation following atomic vapor deposition.<sup>1</sup> On the other hand, atomic manipulation with the STM (Refs. 2 and 3) constitutes a well controlled route for nanofabrication, and arrays of clusters have been produced by moving the tip to the desired cluster positions. The strength of the interaction between a cluster and a surface can be measured with the atomic force microscope.<sup>5</sup> Another recent method for nanostructure fabrication is the direct controlled deposition of nanoclusters from the gas phase. In this case the nature of the constituent atoms of the cluster and surface is essential for characterizing the outcome of the deposition event.<sup>6,7</sup> For different kinetic energies of the impinging clusters the type of processes ranges from soft-landing to fragmentation, implantation, and radiation damage, as experiments<sup>4</sup> and molecular-dynamics (MD) simulations<sup>8-12</sup> show. Apart from nanostructure fabrication, cluster impact constitutes an efficient method to grow thin films<sup>13</sup> in which case the time for nucleation aggregation in the usual atomic deposition is substituted by the time of arrival of the clusters preformed in the gas phase.

In this work we study the deposition of small copper and gold clusters on a Cu(001) surface by constant energy molecular-dynamics simulations. Semiempirical potentials are used to describe the interatomic interactions. The clusters considered have 13 and 55 atoms, and their initial kinetic energies are varied between zero and a few electronvolts per atom. Flat substrates at temperatures of 0, 300, and 800 K have been considered as well as substrates with steps one and two monolayers high. The questions of interest for us are the time spent by the cluster in rearranging from its initial free equilibrium shape to reach its final structure on the substrate, and the dependence of this final structure with the substrate

temperature and the initial cluster velocity. The substrate temperature  $T=800$  K is high compared to usual temperatures in deposition experiments. Nevertheless, this temperature will serve us to study the cluster rearrangements in a high-temperature limit in which the vibrational motion of the surface atoms is important. The details of the calculation are described in Sec. II and the results are presented and discussed in Sec. III.

### II. COMPUTATIONAL METHOD

The Cu(001) surface is modeled as a molecular-dynamics (MD) cell composed of ten atomic layers, each of them containing 128 atoms. Periodic boundary conditions are used in the directions parallel to the surface, while, for the perpendicular direction, three bottom layers of fixed atoms constitute the cell boundary. The atoms are allowed to interact through a many-body potential derived from tight-binding (TB) ideas.<sup>14,15</sup> When there is only one type of atom in the system, the potential takes the form

$$V = \frac{1}{2} \sum_{i=1}^N \left[ \sum_{j=1}^N A e^{-p(r_{ij}/r_0-1)} - \left( \sum_{j=1}^N \xi^2 e^{-2q(r_{ij}/r_0-1)} \right)^{1/2} \right], \quad (1)$$

where the first term is the repulsive pair-potential term and the second is the attractive band-energy contribution.  $N$  is the number of atoms,  $r_{ij}$  is the distance between atoms  $i$  and  $j$ , and  $r_0$  is a reference value (usually the equilibrium distance in the bulk metal). The band-energy term is proportional to the square root of the second moment of the local density of states, which is a measure of the width of the electronic band. The parameters  $\xi$ ,  $A$ ,  $q$ , and  $p$  are usually fitted to reproduce the bulk elastic constants, the cohesive energy, and the lattice parameter of the given metal. The generalization to two types of atoms is simple.<sup>16</sup> We use the values of the parameters given in Ref. 17 for the Cu-Cu, Cu-Au, and Au-Au atomic pairs, which were fitted to the bulk properties of the two metals and of the ordered AuCu<sub>3</sub> alloy. A cutoff radius is used for the potential, which accounts for interactions up to fifth nearest neighbors. To fix the dimensions of the MD cell, or in other words, the lattice parameter of the

substrate for each one of the temperatures, we use the experimental thermal expansion coefficient (this value is close to the theoretical one for the interatomic potential used in this work<sup>17</sup>). The copper substrate is first equilibrated at the three temperatures of interest, namely 0, 300, and 800 K, whereas the free clusters are assumed initially in internal equilibrium at 0 K. The experimental melting point of bulk Cu is 1358 K, so we are still far from it. Furthermore, Loisel *et al.* have used the TB potential in simulations of some surface properties of copper. From the atomic mean-square displacements as a function of temperature and using Lindemann's law, one obtains from their results a melting temperature of about 1250 K.<sup>18</sup> The initial geometries of the Cu and Au clusters correspond to the most stable isomer for a free cluster whose atoms interact with the potential of Eq. (1).<sup>16</sup> These correspond to Mackay icosahedra made up of one and two concentric shells, for 13 and 55 atoms, respectively.<sup>19</sup> Those structures are rather common for free clusters of different elements.<sup>20</sup> After independent equilibration of the two separated subsystems, the cluster is placed close to the Cu(001) surface, at a distance such that the minimum separation between the atoms of cluster and substrate is about 3.8 Å (notice that the nearest-neighbor distance in bulk Cu is 2.56 Å). The orientation of the cluster with respect to the Cu surface is such that an axis through two opposite vertices of the icosahedron is perpendicular to the surface and passes through a four-coordinated interstice of the Cu(001) surface. Simulations are performed with zero initial velocity of the cluster and also with a finite velocity in the direction perpendicular to the surface. Starting with those initial conditions, the Newton equations of motion are integrated up to a maximum of several hundred of ps by using a time step of 2 fs.

We have used different types of indicators to characterize the rearrangement of the cluster on the Cu surface. The first one concerns the time evolution of the temperatures of cluster and substrate, defined from the separate kinetic energies of these two subsystems relative to their respective centers of mass and averaged over 200 time steps (this corresponds to about five periods of vibration, obtained from the bulk Debye frequency). We notice that, once the cluster atoms are tagged at the beginning of the simulation, these are considered to be cluster atoms during the evolution, even if the cluster dismembers. The artificial distinction between cluster and substrate temperatures is intended only as a useful tool that helps to understand the evolution of the deposited cluster. The second indicator refers to partial potential energies, accounting for the interaction between atoms within selected parts of the system. However, due to the many-body character of the potential, the partitioning of the total energy of the system (cluster plus substrate) into a cluster energy, a substrate energy, and a cluster-substrate interaction energy is not uniquely defined. We choose, then, to call partial cluster (substrate) energies to the potential energies of the isolated cluster (substrate) subsystem calculated for the configuration that the cluster (substrate) adopts in the interacting total system, that is,

$$V_{\text{clus}} = \frac{1}{2} \sum_{i=1}^{N_{\text{clus}}} \left[ \sum_{j=1}^{N_{\text{clus}}} A e^{-p(r_{ij}/r_0-1)} - \left( \sum_{j=1}^{N_{\text{clus}}} \xi^2 e^{-2q(r_{ij}/r_0-1)} \right)^{1/2} \right], \quad (2)$$

$$V_{\text{sub}} = \frac{1}{2} \sum_{i=1}^{N_{\text{sub}}} \left[ \sum_{j=1}^{N_{\text{sub}}} A e^{-p(r_{ij}/r_0-1)} - \left( \sum_{j=1}^{N_{\text{sub}}} \xi^2 e^{-2q(r_{ij}/r_0-1)} \right)^{1/2} \right]. \quad (3)$$

The difference between the potential energy  $V$  of the total system and the energies of the two (cluster and substrate) subsystems (as defined above) is called the interaction energy:

$$V_{\text{inter}} = V - V_{\text{clus}} - V_{\text{sub}}, \quad (4)$$

where  $V$  is the total potential energy.  $V_{\text{inter}}$  is analyzed to show explicitly the development of the bonding between the two subsystems. The atomic rearrangements in the cluster, from its initial configuration up to the stage when a rather flat configuration on the substrate has been achieved, are also followed through by using a structural parameter defined as

$$\lambda = \frac{1}{2N_{\text{clus}}} \sum_{i=1}^{N_{\text{clus}}} \left[ \cos\left(\frac{4\pi x_i}{a_0}\right) + \cos\left(\frac{4\pi y_i}{a_0}\right) \right], \quad (5)$$

where  $a_0$  is the bulk lattice parameter of the substrate and  $(x_i, y_i)$  are the coordinates of atom  $i$  in the plane parallel to the surface. Then, for a fcc arrangement in that plane and with the same lattice parameter of the bulk, the value of  $\lambda$  is 1, and smaller than 1 otherwise, so  $\lambda$  gives information on the degree of epitaxy achieved. The same parameter was used by Verlet<sup>21</sup> in establishing a criterion for bulk melting, the value of  $\lambda$  being 1 for a solid and oscillating around 0 for a liquid. A reference structural parameter for the substrate will be considered by extending the sum in Eq. (5) over the substrate atoms in the MD cell. The values of  $\lambda$  given in the section of results below are averages over 200 time steps.

### III. RESULTS

#### A. Deposition of Cu<sub>13</sub>

The Cu<sub>13</sub> cluster is initially released with zero kinetic energy in the proximity of the surface and the cluster-substrate interaction is then switched on. Immediately the cluster starts to approach the substrate driven by the attractive potential, which leads to an increase of the cluster-substrate binding energy. Since we perform constant energy MD simulations in a finite cell with periodic boundary conditions, this energy is invested in raising the cluster and substrate temperatures. Figure 1 shows the evolution of those temperatures as a function of time, for three initial substrate temperatures of 0, 300, and 800 K. The variation in temperature is more noticeable in the cluster than in the substrate. During the first few picoseconds the cluster is strongly heated up and it cools down rapidly afterwards, reaching a temperature close to that of the substrate in a few (5–10) picoseconds. We name this time interval the transient time. However, the fluctuations in the internal temperature of the cluster are large and, except for  $T=0$  K, these do not show a trend to decay in the first 40 ps of the simulation. This behavior is due to its finite number of atoms. In Fig. 2 we show the evolution of the partial and interaction potential energies during the first 40 ps of the simulations. The significant changes occur for  $V_{\text{clus}}$  and

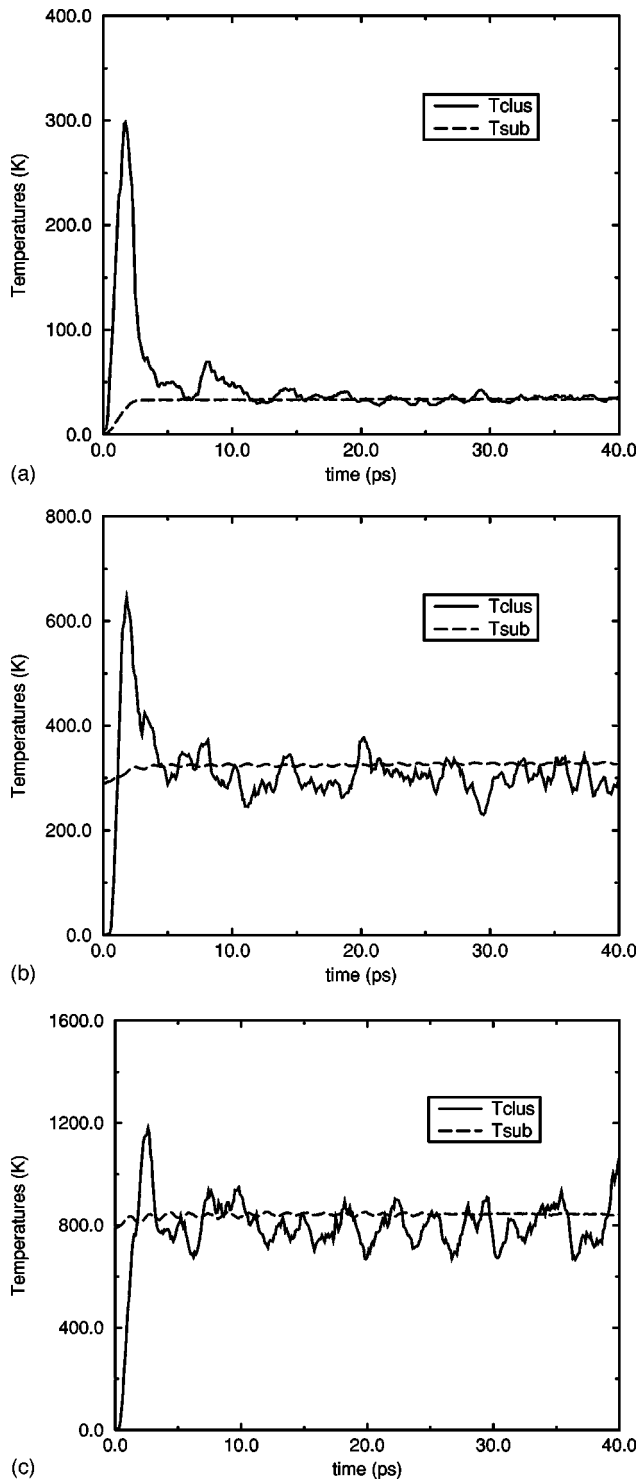


FIG. 1. Cluster and substrate temperatures as a function of time for deposition of  $\text{Cu}_{13}$ . Substrate initially at  $T=0$  K (a), at  $T=300$  K (b), and at  $T=800$  K (c).

$V_{inter}$ . The first one becomes less negative because the initial configuration is the minimum energy structure of the isolated cluster. When the cluster approaches the substrate, the geometrical configuration changes, and consequently its potential energy, calculated in Eq. (2) as if it were an isolated cluster, increases. The fact that the values of  $V_{clus}$  are always less negative than  $V_{sub}$  reflects the smaller average atomic coordination in the cluster. On the other hand it is easy to

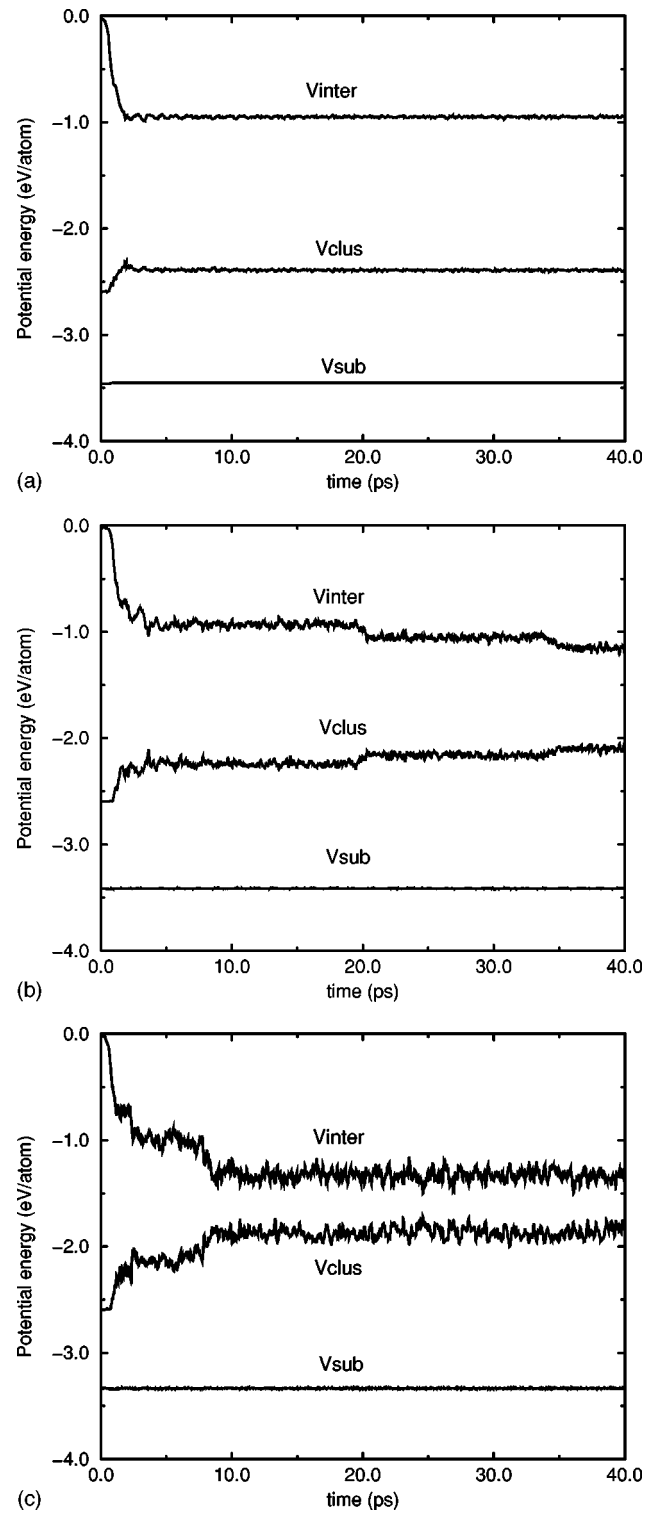


FIG. 2. Time evolution of the partial and interaction potential energies for deposition of  $\text{Cu}_{13}$ . Substrate initially at  $T=0$  K (a), at  $T=300$  K (b), and at  $T=800$  K (c).

understand the behavior of  $V_{inter}$  as the result of the progressive formation of more bonds between the cluster atoms and the substrate as time progresses. The main changes in  $V_{clus}$  and  $V_{inter}$  occur during the transient time in which cluster and substrate temperatures are far from equilibrium (see Fig. 1), and  $V_{clus}$  and  $V_{inter}$  vary slowly afterwards. This means that the main rearrangements of the cluster atoms occur very fast,

and in fact after the transient time, atomic layering parallel to the surface (more than one layer, in general) is distinguished in the cluster structure for the three substrate temperatures considered. The cluster atoms have reached a strong degree of epitaxial arrangement on top of the surface in the case of initial substrate temperature  $T=0$  K. This is shown in Fig. 3(a), where one sees that the structural parameter  $\lambda$  reaches values higher than 0.9. This is not exactly 1 because of thermal effects, which also affect  $\lambda(\text{substrate})$  although to a smaller extent. The initial value of  $\lambda(\text{cluster})$  is negative. This is an effect due to the small number of atoms. For this reason,  $\lambda(\text{cluster})$  is sensitive to the choice of the origin of the coordinate system, in the regime far from epitaxial. In our case, the origin of the coordinate system is in one corner of the MD cell. But as soon as the cluster spreads over the substrate and reaches the epitaxial regime,  $\lambda(\text{cluster})$  takes the expected value close to 1. A very fast epitaxial rearrangement was also obtained for  $\text{Na}_8$  on  $\text{Na}(110)$  from *ab initio* calculations.<sup>7</sup> The thermal atomic vibrations around their equilibrium positions are reflected in progressively smaller values of  $\lambda(\text{substrate})$  for increasing substrate temperatures, as shown in Figs. 3(b) and 3(c). Those temperatures have a stronger effect on  $\lambda(\text{cluster})$  because the cluster atoms, apart from vibrating, also diffuse. The increase of the number of bonds with the substrate during cluster spreading is evidenced by jumps in  $V_{\text{inter}}$  and  $V_{\text{clus}}$  at certain times [see Fig. 2(b), especially]. For an initial substrate temperature  $T=0$  K, only a steep initial change occurs during the transient regime, and the cluster remains effectively frozen afterwards, thermal atomic diffusion being suppressed. However, for a warm or hot substrate, thermal diffusion occurs after the transient. The structural cluster changes begin with the flattening of its bottom half, whose atoms are the nearest to the substrate, to form an adlayer. Cluster atoms from the upper half can then diffuse to the adlayer boundary and step down to increase the adlayer size, or, alternatively, the adlayer can spread and embed the upper atoms. These processes occur at a speed that depends on the substrate temperature and the activation energy for the given process. Consequently, the complete flattening of the cluster to form a two-dimensional island is faster the higher the substrate temperature. As an illustration, we give in Fig. 4 snapshots for the cluster structures after 10 ps for the three substrate temperatures. Only three of the ten substrate layers used are shown in the snapshots along the paper. At 800 K the cluster has evolved to form a two-dimensional island already at 10 ps. The island is not static and its shape changes in time. This also contributes to the reduced values of  $\lambda(\text{cluster})$  in Fig. 3(c). Nevertheless, within our simulation time (40 ps) the island does not lose atoms. At 300 K, the cluster still forms two layers after 10 ps, but atoms of the top layer diffuse afterwards, falling to form part of the first layer, and this becomes reflected in the changes of the interaction energy of Fig. 2(b) at about 20 and 32 ps. For  $T=0$  K, we have the limiting case in which the cluster flattening is the lowest. Consistently with those facts, the changes in  $V_{\text{inter}}$  and  $V_{\text{clus}}$  occur during the first few picoseconds for substrate temperatures  $T=0$  K and  $T=800$  K, in the first case because diffusion is suppressed afterwards, and in the second because the flattening is already complete. In contrast, for  $T=300$  K, important changes of  $V_{\text{clus}}$  and  $V_{\text{inter}}$  occur at times around 20 and 32 ps and changes would

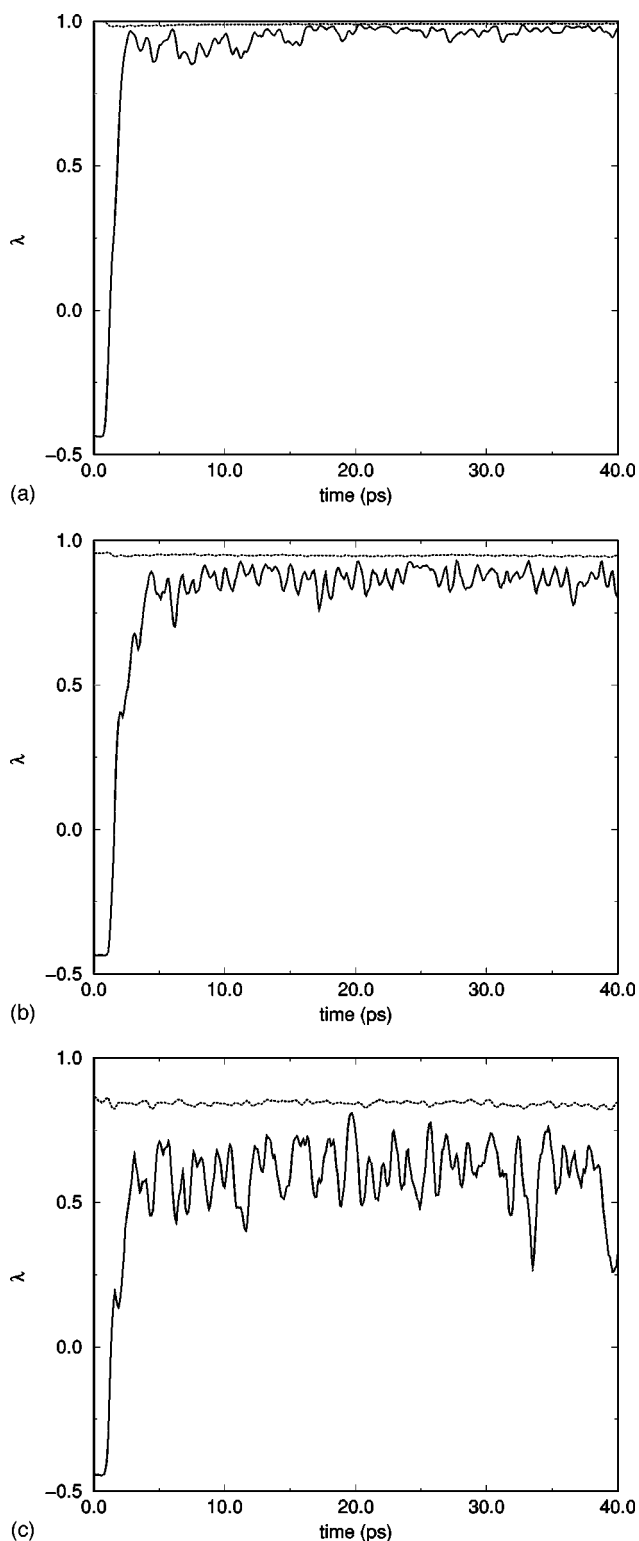


FIG. 3. The time evolution of the lambda function, for  $\text{Cu}_{13}$  (continuous line) and substrate (dotted line). Substrate initially at  $T=0$  K (a), at  $T=300$  K (b), and at  $T=800$  K (c).

presumably occur again at later times beyond our simulation times. Thus, the evolution of the cluster after deposition at zero initial velocity depends very much upon the substrate temperature.

Xie<sup>22</sup> has performed MD simulations for a  $\text{Cu}(100)$  surface using the embedded-atom method of Daw, Foiles, and Baskes.<sup>23,24</sup> At  $T=800$  K, a solid-liquid coexistence occurs:

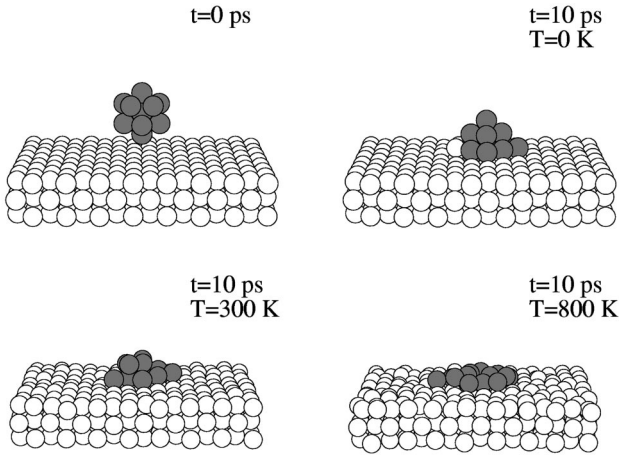


FIG. 4. Snapshots of the structure of  $\text{Cu}_{13}$  10 ps after deposition at different substrate temperatures. The starting configuration is also shown. Dark and light atoms are cluster and substrate atoms, respectively.

the surface layer and the one behind are premolten while the others remain solid. In our case the surface is still solid at this temperature, and the reason is the different many-body potentials used. In fact, the calculated values of the structural parameter  $\lambda$  restricted to the two top layers show the solid character of the surface. The lowest value of  $\lambda$  corresponds to the outermost layer and it is around 0.7 at  $T=800$  K. This is also seen in previous calculations for small clusters of noble metals ( $\text{Cu}_{13}$ ,  $\text{Ag}_{13}$ ,  $\text{Au}_{13}$ ),<sup>16,25,26</sup> which show that cluster melting temperatures are larger for the tight-binding potential of Eq. (1), compared to the embedded atom. On the other hand, the effective-medium theory does not predict any surface melting for  $\text{Cu}(001)$  at 800 K in agreement with the present work.<sup>27</sup>

We next consider the cluster deposited with initial center-of-mass velocities up to  $20 \text{ \AA}/\text{ps}$  (energy of 1.32 eV/atom) normal to the surface. The main difference with respect to the previous results consists in an enhanced and more rapid heating of the cluster during the transient time. Consequently, the cluster is more flat after the transient time compared to the case of zero initial velocity. To illustrate this effect we compare the cluster structures for depositions with initial velocities of zero and  $20 \text{ \AA}/\text{ps}$  and substrate temperature  $T=0$  K. After 10 ps the cluster with zero initial velocity has achieved a structure of three layers (see Fig. 4) whereas for an initial velocity of  $20 \text{ \AA}/\text{ps}$  it reaches a structure of only two layers, with three atoms in the upper one. Thus, the structure that the cluster adopts after the transient, for an initial cluster velocity of  $20 \text{ \AA}/\text{ps}$ , is similar to the one obtained by zero velocity deposition on a warmer substrate at 300 K. Betz *et al.*<sup>11</sup> have studied the local heating of the substrate in the region of cluster impact. For an impact energy of 0.5 eV/at, they find local heatings equivalent to an increase in  $T$  close to 200 K, which is consistent with our finding. Rongwu *et al.*<sup>10</sup> report results for the simulation of the deposition of  $\text{Cu}_{13}$  on a  $\text{Cu}(001)$  surface with initial cluster kinetic energies of 5 and 20 eV/atom, which correspond to cluster velocities of 40 and  $80 \text{ \AA}/\text{ps}$ , respectively, much larger than the velocities in our work. They find that the surface first deforms and then reconstructs after the collision, and the time for the reconstruction is of the same order of

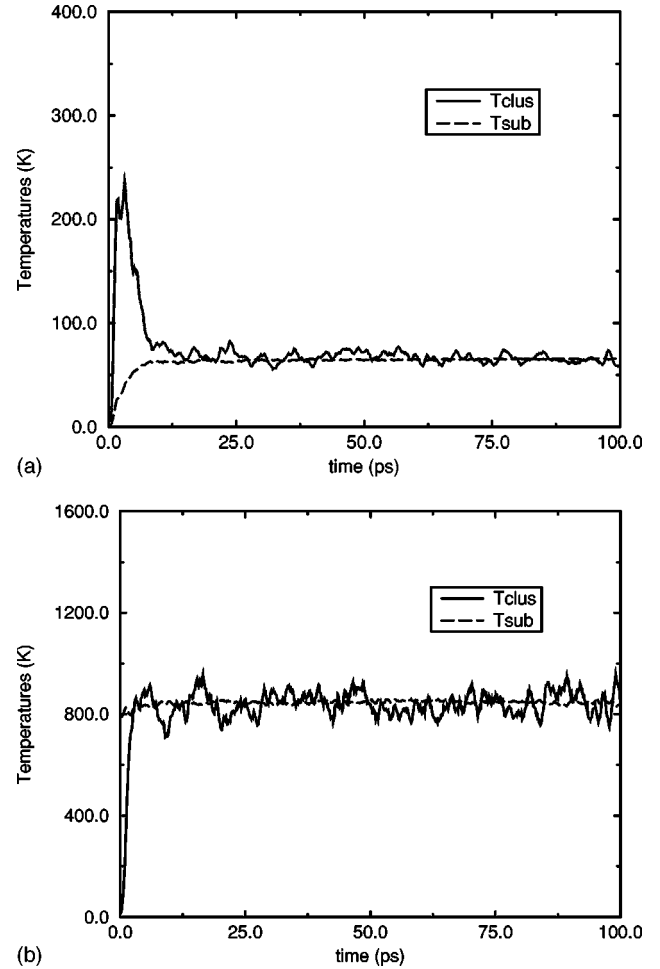


FIG. 5. Cluster and substrate temperatures as a function of time for deposition of  $\text{Cu}_{55}$ . Substrate initially at  $T=0$  K (a) and at  $T=800$  K (b).

magnitude as the time we obtain for cluster-substrate temperature equilibration. We have found that for initial velocities between 20 and  $25 \text{ \AA}/\text{ps}$ , the processes evolve from simple cluster deformation without substantial substrate penetration up to the case where the cluster penetrates into the substrate and it rebounds partially mixed with substrate atoms.

## B. Deposition of $\text{Cu}_{55}$

Figures 5, 6, and 7 show the relevant magnitudes for the deposition of  $\text{Cu}_{55}$  with zero initial kinetic energy: partial temperatures, potential energies, and  $\lambda$ . Comparing with the case of  $\text{Cu}_{13}$ , more atoms have to be reaccommodated on the surface. As a consequence, for a substrate temperature of 0 K the time required to equilibrate the cluster and substrate temperatures is larger (approximately double). After 10 ps, a structure of four layers is formed (see the snapshot in Fig. 8) with a lower degree of epitaxy compared to  $\text{Cu}_{13}$ , as is observed by comparing  $\lambda$  of Figs. 7(a) and 3(a). The cluster keeps the structure of four layers for the rest of the simulation (see Fig. 8). At the substrate temperature  $T=800$  K the situation is completely different, as we observe in Figs. 8 and 9. In this case the structure changes in time with a progressive flattening of the cluster. The transition from four shells

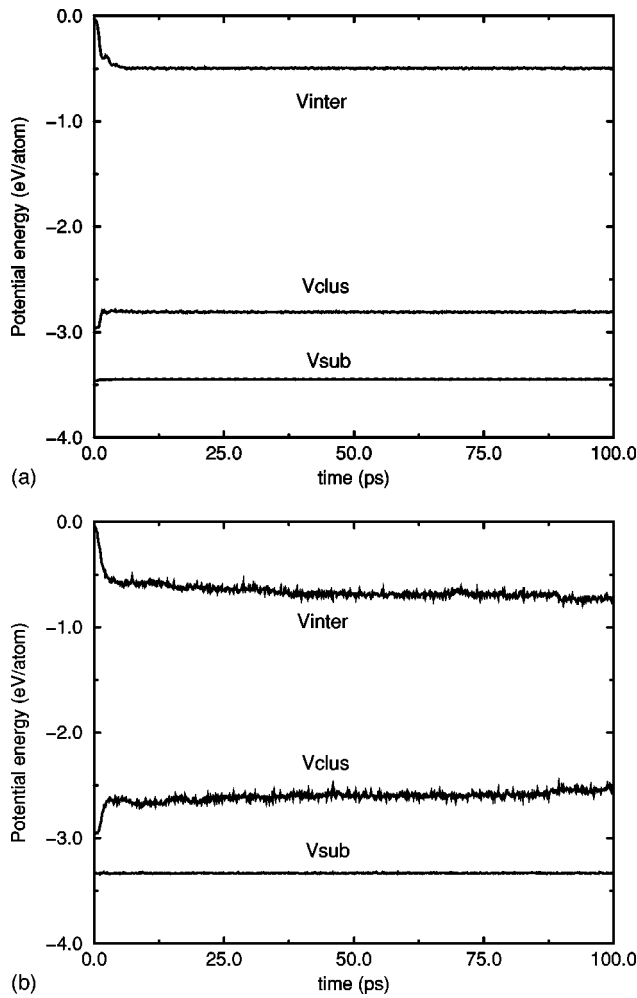


FIG. 6. Time evolution of the partial and interaction energies for deposition of  $\text{Cu}_{55}$ . Substrate initially at  $T=0$  K (a) and at  $T=800$  K (b).

to three shells between 30 and 40 ps is displayed in Fig. 9. The three top atoms in the structure at 30 ps roll down towards the substrate and their respective positions at 80 and 100 ps are shown in the last two snapshots. Those three atoms are represented by dark spheres. The evolution of the cluster structure causes the potential energies in Fig. 6(b) to have a nonzero slope different from the corresponding curves at 0 K in Fig. 6(a). We have extended the simulation up to 400 ps in order to follow the structural evolution of the cluster. A two-shell morphology is reached after 150 ps, with 22 cluster atoms in the top layer and 33 in the bottom layer, two of them exchanged with substrate atoms. Still at the end of the simulation the cluster was formed by two layers, with 15 atoms in the top one. The bottom layer has 40 atoms, three of them coming from exchanges with substrate atoms. An interesting observation is that, at  $T=800$  K,  $\lambda(\text{cluster})$  is a little larger for  $\text{Cu}_{55}$  compared to  $\text{Cu}_{13}$ , and the fluctuations are smaller. A plausible reason is that the ratio of border atoms to island atoms is smaller, so the changes in the shape of the island have a lower effect on  $\lambda(\text{cluster})$ .

### C. Deposition of Au clusters

For deposition of gold clusters on the same Cu surface, the larger mass with respect to copper makes the atomic

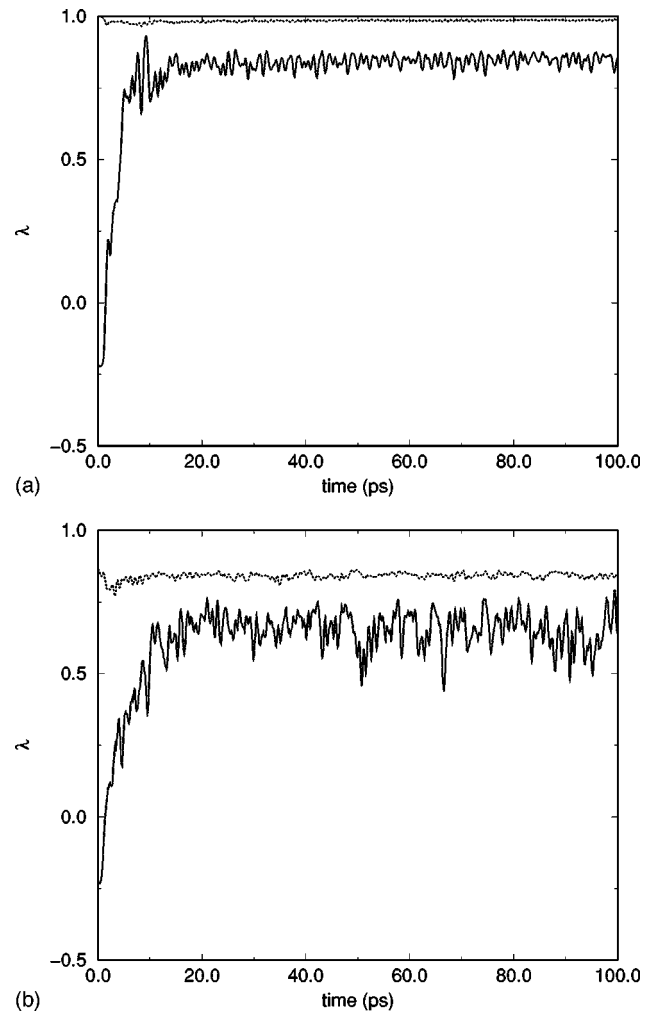


FIG. 7. The time evolution of the lambda function for  $\text{Cu}_{55}$  (continuous line) and substrate (dotted line). Substrate initially at  $T=0$  K (a) and at  $T=800$  K (b).

diffusion processes slower. On the other hand, one can expect strong chemical interactions between the Cu and Au atoms, considering that the binding energy of the Cu-Au dimer is 1.3 times that for the Cu-Cu dimer for the interatomic potential used in this work. We compare the cluster morphologies after 40 ps for deposition of  $\text{Cu}_{55}$  and  $\text{Au}_{55}$

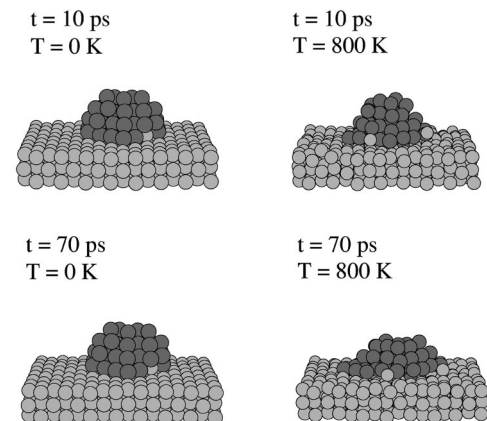


FIG. 8. Snapshots of the structure of  $\text{Cu}_{55}$  10 ps and 70 ps after deposition at substrate temperatures of  $T=0$  K and  $T=800$  K.

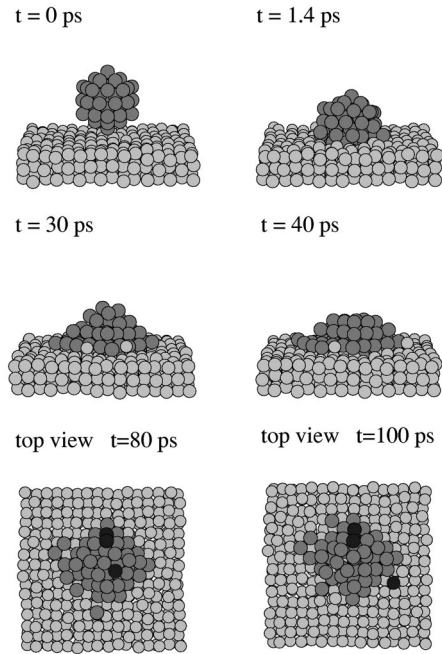


FIG. 9. Snapshots of the structure of  $\text{Cu}_{55}$  for different times after deposition at a substrate temperature  $T=800$  K.

with zero initial velocity on a substrate at 800 K. This temperature has been chosen to facilitate possible mixing between substrate atoms and cluster atoms to form a surface alloy. In the two cases,  $\text{Cu}_{55}$  and  $\text{Au}_{55}$ , the island is formed by three atomic layers, but it appears that the gold cluster spreads and flattens faster than the copper cluster. For  $\text{Au}_{55}$ , a single atom sits on the top layer of the island, 17 are in the middle layer and 37 in the bottom one (one of them is a Cu atom that comes from an exchange event). For  $\text{Cu}_{55}$ , there are 6, 18, and 31 atoms in the top, middle, and bottom layers, respectively (two atoms of the bottom layer come from exchanges with the substrate). We then conclude that exchanges between Au and Cu atoms are few at that temperature, at least within the 40 ps of our simulation, and that a higher cluster kinetic energy would be the only way to promote alloying (work is in progress to study this effect). The faster spreading is a direct consequence of the stronger interaction of  $\text{Au}_{55}$  with the copper substrate. In spite of the different lattice constants of bulk Cu and Au metals, the Au island that forms on top of the Cu surface retains the same interatomic distances of the substrate.

#### D. Deposition of $\text{Cu}_{13}$ at steps

We have studied the deposition of  $\text{Cu}_{13}$  on steps one and two monolayers high of the same Cu(001) surface at  $T=0$  K. The cluster was initially in a symmetrical position above the step edge. Figure 10 shows the starting configurations and the configurations after 20 ps. The clusters immediately wet the region of the step, and in our simulation at  $T=0$  K, the clusters remain frozen afterwards. Figure 11 compares the interaction energies  $V_{\text{inter}}$  for the flat and the stepped cases. There is a substantial enhancement of the binding to the substrate mediated by the steps, and this is due to the higher atomic coordination available at the step edge. This allows us to predict that steps will provide anchoring sites for clus-

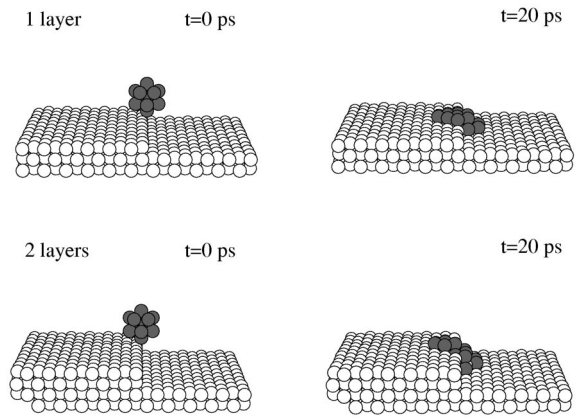


FIG. 10.  $\text{Cu}_{13}$  deposited on stepped surfaces at  $T=0$  K. Upper: snapshots at  $t=0$  and  $t=20$  ps for one-layer step. Lower: snapshots at  $t=0$  and  $t=20$  ps for two-layer step. Dark and light atoms are cluster and substrate atoms, respectively.

ters diffusing over surfaces containing planar terraces separated by steps, in agreement with recent experimental findings.<sup>28</sup>

#### IV. CONCLUSIONS AND COMMENTS

In this paper we have studied the atomic rearrangements that take place when Cu and Au clusters of negligible or very small kinetic energy are deposited on a Cu(001) surface. For this purpose we have performed constant energy classical molecular-dynamics simulations for the substrate at three different initial temperatures,  $T=0$  K, 300 K, and 800 K. For  $T=0$  K, the atomic rearrangements occur in the first few picoseconds of the simulation, and the cluster remains frozen afterwards in a metastable configuration. For Cu-cluster deposition, this metastable configuration is flat, although formed by more than one layer, and it shows a high degree of epitaxy on the substrate lattice. At medium and high substrate temperatures, in addition to the initial short-time rearrangement there is a further flattening of the cluster due to thermal diffusion of atoms. At  $T=800$  K, the vibrational

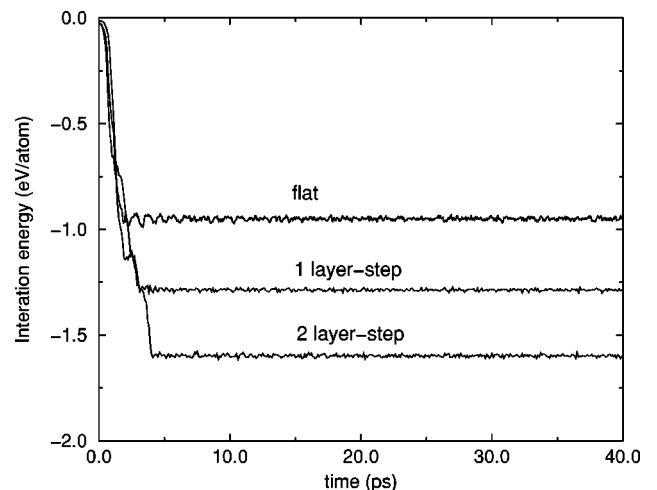


FIG. 11. The development of the binding of  $\text{Cu}_{13}$  cluster to the substrate for the cases of flat and stepped surfaces (one-layer step and two-layer step) at  $T=0$  K.

motion of both substrate and deposited cluster is substantial. In addition, the shape of the island changes in time. For Au clusters deposited under similar conditions the results are rather similar. Exchanges between cluster and substrate atoms are very few for our simulation times, and higher cluster kinetic energies appear to be required for surface alloying to occur. Simulations of the deposition of Cu<sub>13</sub> onto a stepped surface indicate the affinity of the deposited atoms for the step edge.

Our study has interest because it is now possible to observe in the laboratory atomistic surface processes down to the level of only one atom.<sup>29</sup> It should be noticed that the characteristic observation times are many orders of magnitude larger than MD simulation times. As a recent example,<sup>30</sup> we mention a field ion microscopy imaging of the structure of a single cluster soft landed on a tip. The authors report that a nanometer size Au cluster spends between seconds and minutes for spreading on the surface of a W tip. Nevertheless, we are confident in predicting qualitative trends: a flattening of the cluster occurs in a few picoseconds, and except at very low substrate temperatures, a single two-dimensional island will form subsequently in the usual

observation times. This, however, should not be extrapolated to other metals without further calculations. For instance, deposition of Ag<sub>7</sub> on Pd(001) leads to cluster fragmentation for an impact energy of 2.9 eV/at.<sup>4,31</sup> On the other hand the plasmon resonance of Ag clusters of about 300 atoms deposited at energies of 1.3 eV/at on a quartz glass surface only reveals deformation of the cluster but not fragmentation,<sup>32</sup> in agreement with our results. These examples indicate the sensitivity of the results to the chemical nature of cluster and substrate. On the other hand, static total energy calculations for many different cluster configurations find the more stable atomic arrangement of an adsorbed cluster.<sup>33,34</sup> Both MD and static calculations are important in order to aid in the interpretation of experiments.

#### ACKNOWLEDGMENTS

This work has been supported by DGES (Grant No. PB95-0720-C02-01) and Junta de Castilla y Leon (Grant No. VA 72/96). F.P. acknowledges support from Junta de Castilla y Leon.

- 
- <sup>1</sup>H. Röder, E. Hahn, H. Brune, J.P. Bucher, and K. Kern, *Nature* (London) **366**, 141 (1993).
- <sup>2</sup>J.I. Pascual, J. Méndez, J. Gómez-Herrero, A.M. Baró, N. García, and V.T. Binh, *Phys. Rev. Lett.* **71**, 1852 (1993).
- <sup>3</sup>R. Ullmann, T. Will, and D.M. Kolb, *Chem. Phys. Lett.* **209**, 238 (1993).
- <sup>4</sup>G. Vandoni, C. Félix, R. Monot, J. Buttet, and W. Harbich, *Chem. Phys. Lett.* **229**, 51 (1994).
- <sup>5</sup>S.P. Jarvis, H. Yamada, S.I. Yamamoto, H. Tokumoto, and J.B. Pethica, *Nature* (London) **384**, 21 (1996).
- <sup>6</sup>H.P. Cheng and U. Landman, *J. Phys. Chem.* **98**, 3527 (1994).
- <sup>7</sup>H. Häkkinen and M. Manninen, *Phys. Rev. Lett.* **76**, 1599 (1996).
- <sup>8</sup>W.D. Luedtke and U. Landman, *Phys. Rev. Lett.* **73**, 569 (1994).
- <sup>9</sup>H. Hsieh, R.S. Averback, H. Sellers, and C.P. Flynn, *Phys. Rev. B* **45**, 4417 (1992).
- <sup>10</sup>L. Rongwu, P. Zhengying, and H. Yukun, *Phys. Rev. B* **53**, 4156 (1996).
- <sup>11</sup>G. Betz and W. Husinsky, *Nucl. Instrum. Methods Phys. Res. B* **122**, 311 (1997).
- <sup>12</sup>C. Massobrio and B. Nacer, *Z. Phys. D* **40**, 526 (1996).
- <sup>13</sup>H. Haberland, Z. Insepov, and M. Moseler, *Phys. Rev. B* **51**, 11 061 (1995).
- <sup>14</sup>F. Ducastelle, *J. Phys. (Paris)* **31**, 1055 (1970).
- <sup>15</sup>R.P. Gupta, *Phys. Rev. B* **23**, 6265 (1981).
- <sup>16</sup>M.J. López, P.A. Marcos, and J.A. Alonso, *J. Chem. Phys.* **104**, 1056 (1996).
- <sup>17</sup>F. Cleri and V. Rosato, *Phys. Rev. B* **48**, 22 (1993).
- <sup>18</sup>B. Loisel, D. Gorse, V. Pontikis, and J. Lapujoulade, *Surf. Sci.* **221**, 365 (1989).
- <sup>19</sup>A.L. Mackay, *Acta Crystallogr.* **15**, 916 (1962).
- <sup>20</sup>J.M. Montejano-Carrizales, M.P. Iñiguez, J.A. Alonso, and M.J. López, *Phys. Rev. B* **54**, 5961 (1996).
- <sup>21</sup>L. Verlet, *Phys. Rev.* **159**, 98 (1967).
- <sup>22</sup>Q. Xie, *Phys. Status Solidi B* **207**, 153 (1998).
- <sup>23</sup>M.S. Daw and M.I. Baskes, *Phys. Rev. Lett.* **50**, 1285 (1983); *Phys. Rev. B* **29**, 6443 (1984).
- <sup>24</sup>M.S. Daw, S.M. Foiles, and M.I. Baskes, *Mater. Sci. Rep.* **9**, 251 (1993).
- <sup>25</sup>C. Rey, L.J. Gallego, J. García-Rodeja, J.A. Alonso, and M.P. Iñiguez, *Phys. Rev. B* **48**, 8253 (1993).
- <sup>26</sup>J. García-Rodeja, C. Rey, L.J. Gallego, and J.A. Alonso, *Phys. Rev. B* **49**, 8495 (1994).
- <sup>27</sup>H. Häkkinen and M. Manninen, *Phys. Rev. B* **46**, 1725 (1992).
- <sup>28</sup>S.J. Carroll, K. Seeger, and R.E. Palmer, *Appl. Phys. Lett.* **72**, 305 (1998).
- <sup>29</sup>A. Götzhäuser and G. Ehrlich, *Phys. Rev. Lett.* **77**, 1334 (1996).
- <sup>30</sup>D. Lovall, M. Buss, R.P. Andres, and R. Reifengerger, *Phys. Rev. B* **58**, 15 889 (1998).
- <sup>31</sup>C. Felix, G. Vandoni, C. Massobrio, R. Monot, J. Buttet, and W. Harbich, *Phys. Rev. B* **57**, 4048 (1998).
- <sup>32</sup>H. Hövel, A. Hilger, I. Nusch, and U. Kreibig, *Z. Phys. D* **42**, 203 (1997).
- <sup>33</sup>A.F. Wright, M.S. Daw, and C.Y. Fong, *Phys. Rev. B* **42**, 9409 (1990).
- <sup>34</sup>H.V. Roy, P. Fayet, F. Patthey, W.D. Schneider, B. Delley, and C. Massobrio, *Phys. Rev. B* **49**, 5611 (1994).